

Review

Critical Review of Low-Temperature CO Oxidation and Hysteresis Phenomenon on Heterogeneous Catalysts

Rola Mohammad Al Soubaihi ¹, Khaled Mohammad Saoud ^{2,*}  and Joydeep Dutta ^{1,*} 

¹ Functional Materials, Department of Applied Physics, The Royal Institute of Technology, School of Engineering Sciences, Isafjordsgatan 22, SE-164 40 Kista, Stockholm, Sweden; rolaas@kth.se

² Liberal Arts and Sciences Program, Virginia Commonwealth University in Qatar, P.O. Box 8095, Doha, Qatar

* Correspondence: s2kmsaou@vcu.edu (K.M.S.); joydeep@kth.se (J.D.);
Tel.: +974-66037810 (K.M.S.); +46-737652186 (J.D.)

Received: 30 October 2018; Accepted: 11 December 2018; Published: 14 December 2018



Abstract: There is a growing demand for new heterogeneous catalysts for cost-effective catalysis. Currently, the hysteresis phenomenon during low-temperature CO oxidation is an important topic in heterogeneous catalysis. Hysteresis provides important information about fluctuating reaction conditions that affect the regeneration of active sites and indicate the restoration of catalyst activity. Understanding its dynamic behavior, such as hysteresis and self-sustained kinetic oscillations, during CO oxidation, is crucial for the development of cost-effective, stable and long-lasting catalysts. Hysteresis during CO oxidation has a direct influence on many industrial processes and its understanding can be beneficial to a broad range of applications, including long-life CO₂ lasers, gas masks, catalytic converters, sensors, indoor air quality, etc. This review considers the most recent reported advancements in the field of hysteresis behavior during CO oxidation which shed light on the origin of this phenomenon and the parameters that influence the type, shape, and width of the conversion of the hysteresis curves.

Keywords: CO hysteresis; self-Sustaining CO oxidation; dynamic catalysis; catalytic activity; catalyst; Isothermal; bi-stability region

1. Introduction

Carbon monoxide (CO) is a toxic gas that is often called the silent killer since it does not have taste, color or smell and generally results from incomplete combustion of fossil fuels. Most of the CO emission occurs due to cold start of vehicles [1–5]. A small exposure to CO can be fatal since it has a high affinity to replace oxygen and binds to hemoglobin in blood cells [6].

Catalytic CO oxidation has gained increasing attention in recent years, primarily due to its demand in industrial processes, such as: pollution reduction in the auto industry, abatement of gaseous waste in petrochemical industries, synthesis of pure gases, ethanol or other fuel production, and pure hydrogen production for proton-exchange membrane fuel cells [7–9]. CO oxidation also has a wide range of diverse applications in long-life carbon dioxide (CO₂) lasers, gas masks, catalytic converters, sensors, indoor air quality improvement, etc. [10–13]. Catalytic CO oxidation has been widely studied, especially for application in automotive industry [14–16]. High operation temperature (>570 K) of the widely used three-way catalytic converters inhibit the conversion of CO and other pollutants during the cold start period. Hence, recent studies have targeted the development of new cost-effective and low-temperature catalysts [17–19].

The CO oxidation reaction is one of the most extensively studied in the history of heterogeneous catalysis. Often, CO oxidation is considered to be an interesting probe reaction for other oxidation

reactions and is an essential reaction for cleaning air and lowering automotive emissions as reported in the web of science database, and the publications on this subject are growing exponentially [20].

Transition metals are widely used to activate surface catalyzed reactions, such as CO oxidation, primarily due to high dissociation probability and very low adsorption energy. Transition metals are characterized by their half-filled d-bands which enables them to have the highest activity compared to other metals. Thus, platinum group metals, such as platinum (Pt), palladium (Pd) and rhodium (Rh), are considered the most efficient transition metal catalysts. They have emerged as most efficient catalysts due to their ability to dissociate molecular oxygen at a low temperature and to bind strongly with both atomic oxygen and CO [21]. Noble metal catalysts are known for their excellent activities, such as water tolerance, and low light-off temperatures [22,23]. Recent studies report that gold (Au) is highly active towards CO oxidation at low temperatures (close to ambient temperature) [24–28] even though single molecule CO conversion are prohibited due to the presence of water [29]. Gold's selective binding to CO and non-selective loose binding to other reactants causes its high activity which may provide sufficient concentration of CO on surfaces, thus lowering the activation energy to a negligible value enabling the reaction to proceed at room temperature [30]. The high activity of gold towards CO oxidation is reported to be maximum for gold particles (<5 nm in size) supported on reducible metal oxides, such as ceria [24], iron oxide, or titania [25,31–36]. CO oxidation reaction with gold catalysts occur at the interface between the gold metal particle and the oxide support, the CO adsorbed on the gold particles and oxygen (O_2) activated from the oxide support [31,33,34,37–39].

Recent studies focus on reducing the high cost of noble metals and improving the stability of catalysts, motivating the investigation for new materials such as Mn, Fe, Co, Ni, Cu or their combinations and concepts to reduce the use of precious metal content to find suitable substitutes for noble metals [40–45]. As the high activity, high selectivity, and long lifetime of the catalysts are a challenge in heterogeneous catalysis, it is crucial to design catalysts with active sites and other features, to render them useful for any specific applications. Although CO oxidation in the presence of O_2 is considered a relatively simple reaction, researchers have proposed over 20 different mechanistic steps occurring during this reaction [46–53]. One of the most acceptable mechanisms for low-temperature CO oxidation is the Langmuir–Hinshelwood (LH) dual-site mechanism, in which the reaction is considered to occur between CO and O_2 after both molecules have been adsorbed on the surface of a catalyst [52,54,55]. One of the most challenging tasks in heterogeneous catalysis is understanding catalysts under conditions of dynamic reaction and investigating the microscopic processes occurring at the surfaces and in the bulk material of solid catalysts during both heating and cooling cycles [56].

CO oxidation has received a great amount of attention in studies on catalytic reaction dynamics due to its rich, dynamic behavior, wherein it exhibits hysteresis behavior, i.e., regions where multiple steady states are observed for a broad range of experimental conditions, such as dynamic behavior with kinetic instabilities, hysteresis effects and self-sustained oscillations [57]. This review highlights the importance of understanding the dynamic behavior of catalytic oxidation of CO for the future development of catalytic CO oxidation systems.

2. Origin of Hysteresis Phenomenon in Low-Temperature CO Oxidation

Hysteresis is defined as the dependence of the state of a system on its history. Hysteresis occurs in many systems, such as in ferromagnetic and ferroelectric systems, as well as in catalytic materials. Hysteresis effects can be a dynamic lag between an input and an output which disappears if the input is varied very slowly; this is often known as rate-dependent hysteresis [58]. This type of hysteresis has a persistent memory of the past state that persists after the transients have died out [59,60]. Adsorption hysteresis is one of the well-known hysteresis that occurs during physical adsorption processes where the quantity adsorbed is different when the gas is being added than when it is being removed. This hysteresis is caused by the differences in the nucleation and evaporation mechanisms inside mesopores, and can be related to other effects, such as cavitation and pore blocking. This effect

was reported in physical adsorption, where hysteresis was influenced by mesopores (2–50 nm) which is associated with the appearance (50 nm) and disappearance (2 nm) of mesoporosity in nitrogen adsorption isotherms as a function of Kelvin radius [61]. Furthermore, the effect of the support during the thermal decomposition hysteresis of palladium oxide (PdO) supported on zirconia (ZrO_2), titania (TiO_2), ceria (CeO_2), and gamma-alumina ($\gamma-Al_2O_3$) was observed and investigated by Farrauto et al. who reported large hysteresis width in thermal resistance of $\gamma-Al_2O_3$ followed by ZrO_2 , and relatively small hysteresis for TiO_2 and CeO_2 , respectively [62].

In heterogeneous catalysis, often temperature hysteresis is observed when the reaction parameter during a complete cycle, such as reaction rate or the degree of conversion, does not match with increasing and decreasing temperatures. As a consequence, a hysteresis loop is created, where the ascending and the descending branches of the conversion (%) vs. temperature plot do not coincide. Hysteresis can also be explained based on the existence of several steady states in a catalytic systems, where, during a gradual temperature change, one steady state is replaced by another state with different kinetic features, reacting to proceed at a different rate for constant reactor temperatures [63–65]. The hysteresis behavior of CO oxidation over Pd/SiO₂ and (Pd + Cr₂O₃)/Al₂O₃ catalysts has been studied experimentally and explained based on the existence of different steady states during reaction [65]. Recent CO oxidation studies during heating followed by cooling cycles have shown hysteresis behavior, with higher conversions during extinction [5,49,52,56,66–73]. Yap et al. described that the ignition-extinction hysteresis occur following the steps listed herein: (1) adsorption of CO at low temperatures; (2) ignition when CO starts to desorb from a catalyst surface; (3) CO and O adsorption on the active sites and surface reactions take place between adsorbed CO and O; (4) trigger an increase in the reaction rate; (5) stability during high reactive state and a balance between heat generation and the heat losses; (6) interaction of the CO more strongly with the surplus oxygen allowed by the oxygen covered surface at high temperatures which enhances reactivity by lowering activation energy; (7) high and stable reaction rate due to the enhanced reactivity between adsorbed CO and the high oxygen coverage as the catalyst temperature drops which gives rise to a hysteresis phenomenon or having two values of reaction rates at the same temperature [74].

During ignition (light-off) and extinction (light-out) exothermic CO oxidation reactions, hysteresis can occur during the conversion as a function of temperature. Consequently, a hysteresis loop can appear because of a mismatch between the activity during the ignition and extinction processes. There are three regions of activity observed: the first region has low activity (before the light-off temperature), where CO is adsorbed on a catalyst surface, followed by a region with high activity at a higher temperature (after the light-off temperature) and finally, a region of bi-stability before the light-out temperature, as shown in Figure 1.

Hysteresis effects in CO oxidation [75,76], as well as methane oxidation reactions, have been reported [77–80]. Several studies report the differences in the activity of CO, NO, C₃H₆, and CH₄ oxidation on Pt and Pd catalysts during the light-off and the light-out [67,77,81–83]. A typical hysteresis behavior for CO oxidation over Pt/Al₂O₃ has been extensively studied and reported [49,53,55,56,84–90]. Simultaneous oxidation of CO and CH₄ on Pt/Al₂O₃ and Pt/CeO₂ results in a reverse hysteresis for methane oxidation [5]. Moreover, CO self-sustained combustion over the Cu-Ce/ZSM-5 or CuCe_{1-x}Zr_xO_y/ZSM-5 catalyst has been reported [91,92]. The explanation of hysteresis effects by multiple steady states has been comprehensively reviewed by Hlaváček et al. [93]. Engel et al. have explained the appearance of a hysteresis loop in CO oxidation on a contaminated platinum wire by removing sulfur and carbon impurities which could affect the reaction on the metal surface [75]. A higher conversion often indicates normal hysteresis behavior during extinction. The higher activity of the catalyst during extinction can be attributed to surface inhibition by CO adsorption, reaction exothermicity, and thermal inertia of the catalyst. Carlsson et al. [5], argued that normal hysteresis occurs due to three possible reasons: (1) kinetic bistability, (2) interaction between reaction kinetics and diffusion phenomenon, and (3) local overheating of catalyst surfaces.

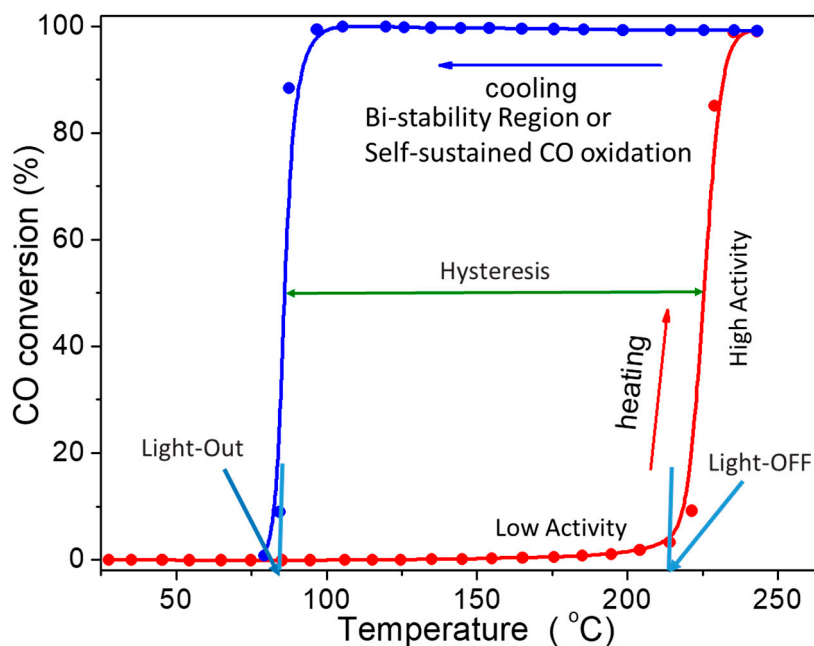


Figure 1. Typical hysteresis can occur during ignition (light-off) and extinction (light-out) exothermic CO oxidation reaction.

CO inverse hysteresis behavior was observed in the case of gas mixtures, such as CO, nitrous oxide (NO) and propane (C_3H_6) mixture, where the catalytic activity during ignition exceeded the activity during extinction. The inverse hysteresis was theorized to occur due to high-temperature oxidation of Pt in the presence of NO or C_3H_6 , to form an oxide phase that is less catalytically active than metallic Pt. Additionally, at low-temperatures, Pt oxide is reduced back to metallic Pt [67]. This behavior is observed for switching of CO hysteresis behavior from normal hysteresis to inverse hysteresis in a CO/NO/ O_2 mixture, which was attributed to reversible oxidation of the Pt surface [67,91]. Inverse hysteresis is also observed for catalysts containing very small Pt- nanoparticles (<2 nm), while typical hysteresis is observed for large Pt- nanoparticles which could be attributed to the different CO adsorption strengths, surface-bulk oxidation of Pt particles, and regeneration of the active sites [94]. Normal hysteresis is observed for the PdCu(110) and Cu-Ce-Zr-O systems [90,95] single crystal alloys, while inverse hysteresis is observed on unsupported catalysts, such as Pd/Ag alloys [96]. Rapid CO adsorption and diffusion is considered crucial for producing strong hysteresis and bistability [97].

Beusch et al. first introduced isothermal multiplicity, such as hysteresis and oscillation in CO oxidation, on Pt-cylindrical catalyst pellets in 1972 [98]. It was argued that hysteresis was independent of the total volumetric flow rate and in-effect related to the multiplicity in the system and is influenced due to the reaction and the chemisorption rates. The results were explained to occur following the Eley-Rideal mechanism with oxygen reacting with adsorbed CO following Langmuir model for adsorption. Multiple steady states could occur when the intrinsic rates of the reaction and chemisorption steps are roughly of equal size [98]. However, theoretical studies suggest that a reactant concentration gradient occurs during reactions in LH models, wherein one of the reactants is strongly adsorbed, leading to isothermal multiplicity [99–101]. As a result, the multiplicity is explained by the interaction of intraparticle diffusion and surface reaction of a sorption step involving at least one strongly adsorbed reactant [99–101].

The hysteresis effects are mostly observed in the oxidation of CO in supported and unsupported metal catalysts [5,52,55,56,98]. Most studies focused on Pt or Pd catalysts supported on alumina [73,102–106] or silica [107,108] substrates. Other studies suggest that diffusion-reaction interactions can lead to multiplicity [69,70]. Eigenberger et al. showed that two or more surface rate steps of roughly equal magnitude could lead to isothermal multiplicity in a gradient-less reactor [109].

In 1978, Cutlip and Kenney were able to explain and revised Beusch's hypothesis to explain their experimental observations [103]. Recent experimental observations suggest that the hysteresis during CO oxidation arises from the diffusion-reaction interaction. Hegedus et al. reported that the increase in the intrapellet diffusion resistances of supported metal catalyst (e.g., Pt/A120 catalyst), upon aging, leads to a significant broadening of the multiplicity region (hysteresis width) agreeing well with transport hypothesis, as suggested by Oh et al. [68]. Chakrabarty et al. explained hysteresis based on the surface reaction–sorption interferences, where sorption of the reactants on the catalyst surface is important to the obtained hysteresis behavior, leading to isothermal multiplicity [56]. Similar observations for multiplicity have been explained; they occur due to the competition of sorption by reactants [98,110,111] and switching of the type of CO complexation on catalyst surface [112] or the interaction of O₂ with chemisorbed CO [113]. This phenomenon could be explained by the alternation between metallic Pt active species and surface-oxidized Pt nanoparticles (NPs). The local CO consumption can lead to the increase or decrease in CO conversion [114,115]. Similar results were reported for P(111) [116]. Subbotin reported that the value of the temperature hysteresis in CO oxidation on copper-cermet catalysts increase with increasing CuO content [117].

Although the hysteresis in CO oxidation over various catalysts have been reported in recent years, a majority of the authors did not propose any original interpretation of this phenomenon. Instead, they attribute the hysteresis phenomenon to the presence of multiple steady states as a necessary condition for hysteresis [114,115]. Frank-Kamenetskii suggested the concept of temperature hysteresis in heterogeneous catalysis based on the macro-kinetic transition from the kinetic to the diffusion mode during hysteresis [118].

Recently, the hysteresis phenomenon was explained to arise due to the existence of some steady states in a catalytic system, phase transitions in catalysts, changes in the surface state of the adsorbed components, and removal of admixtures from a catalyst surface that can hinder the reaction. Subbotin et al. explained the hysteresis effect based on the exothermic heterogeneous catalytic reaction upon reaching a particular reaction rate; the amount of heat liberated at an active reaction center becomes too large to be dissipated in the environment [119,120]. Generally, this is due to the poor heat conductivity of porous oxide supports or poor active centers of inactive catalytic mass. As a result, the actual reaction temperature of the active center is higher than the average temperature of the catalyst bed, leading to local overheating of the active centers and thus a higher conversion than expected at the measured temperature. After the heating is turned off, the excessive heat requires a longer time to dissipate due to poor heat removal, maintaining an actual temperature of the active centers that are higher than the temperature measured by a thermocouple [119,120]. The local overheating of active sites as a result of the liberation of excessive heat during the highly exothermic reaction of the CO oxidation into CO₂ leads to a catalyst remaining active at lower temperatures during extinction [71,121]. The formation of hysteresis loops in CO oxidation has also been attributed to CO island formation by some authors [30].

Kipnis explained the role of reaction exothermicity and nanometer-scale particle size of CO oxidation on supported Au- nanoparticles and explained the jump of conversion as a result of temperature variation, CO conversion hysteresis, appearance of a hot spot, and precursor self-activation because of sharp decrease in apparent activation energy of the catalyst and the exothermicity of CO oxidation which brings the reaction into an external diffusion control regime [122–124]. Similar results were reported for the hysteresis in preferential CO oxidation over a ceria-supported catalyst containing 0.28 wt% Au and germanium (Ge) and gadolinium (Gd) dopants which was attributed to catalyst activation [97]. It was reported that the “direction” of the hysteresis depended on the CO partial pressure [120,125].

3. Effect of Catalysts and Reaction Parameters/Conditions on Hysteresis Behavior

In a catalytic reactor, inlet temperature, gas pressure, particle size, type and nature, inlet gas composition and reactant concentration affect the performance of a catalyst [126]. Casapu et al.

investigated Pt particle size distribution on the hysteresis during CO oxidation over Pt/Al₂O₃ and found that hysteresis is strongly dependent on the particle size of the catalyst. Inverse hysteresis is observed for catalysts containing very small Pt- nanoparticles (< 2 nm), and normal hysteresis for large Pt- nanoparticles, which was attributed to the different surface/bulk CO adsorption strength, oxidation of Pt- nanoparticles, the catalyst active sites regeneration and the exothermicity of the CO oxidation reaction (Figure 2) [94].

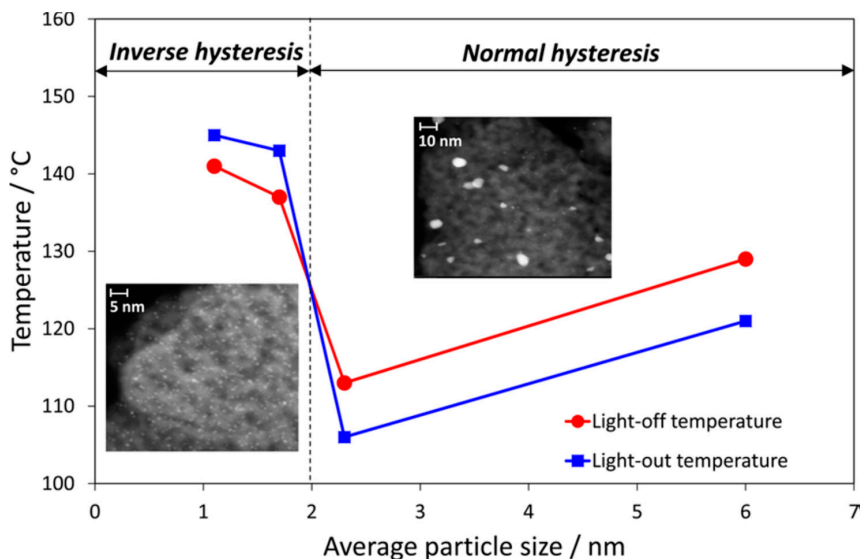


Figure 2. Light-off and light-out temperatures vs. average Pt particle size during CO oxidation [94].

The inlet gas stoichiometric ratio of CO and O₂ has also been investigated and recent data shows that it could affect the conversion profile and the dynamic behavior of a catalyst [127]. Newton reported that hysteresis effect is dependent on the ratio between O₂/CO during CO oxidation over Pt surfaces and supported catalysts, such as Pt/Al₂O₃, and the optimum ratio were (1 < O₂/CO < 5) [127].

Most of the reviewed literature reported the effect of CO concentrations at different inlet temperature on hysteresis behavior [77,128–134]. The width of the hysteresis loop was larger for higher CO concentrations, as shown in Figure 3.

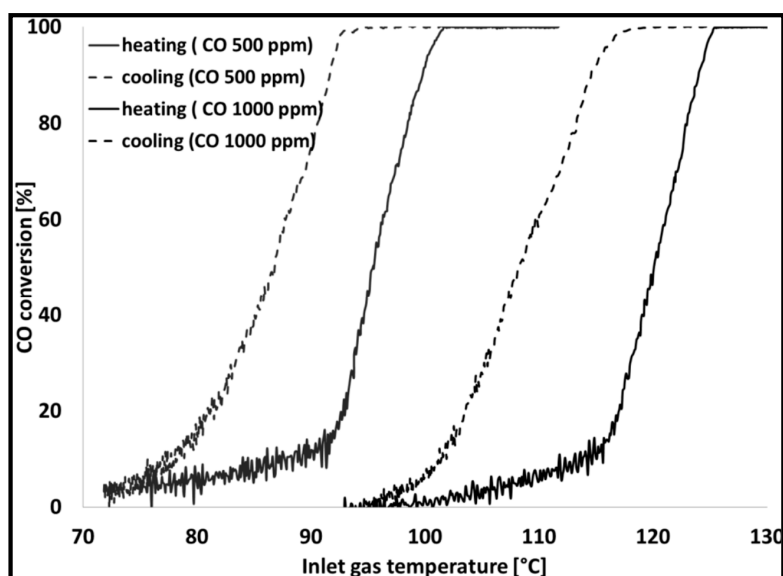


Figure 3. Temperature-programmed CO oxidation with the following inlet conditions: 1000 ppm or 500 ppm CO, 10% H₂O, 10% CO₂, and 10% O₂ over a Pt/Al₂O₃ monolith [77].

Subbotin et al. studied CO oxidation hysteresis behavior on Pt foil and CuO and found that the hysteresis is wider for the CuO catalysts, which could be attributed to the higher activity in CuO catalysts as compared to that on the Pt foil. Figure 4 shows the study of hysteresis phenomenon on unsupported CuO prepared by the decomposition of Cu hydroxycarbonate, which is one of the most active catalysts for this reaction on Pt-foil [63].

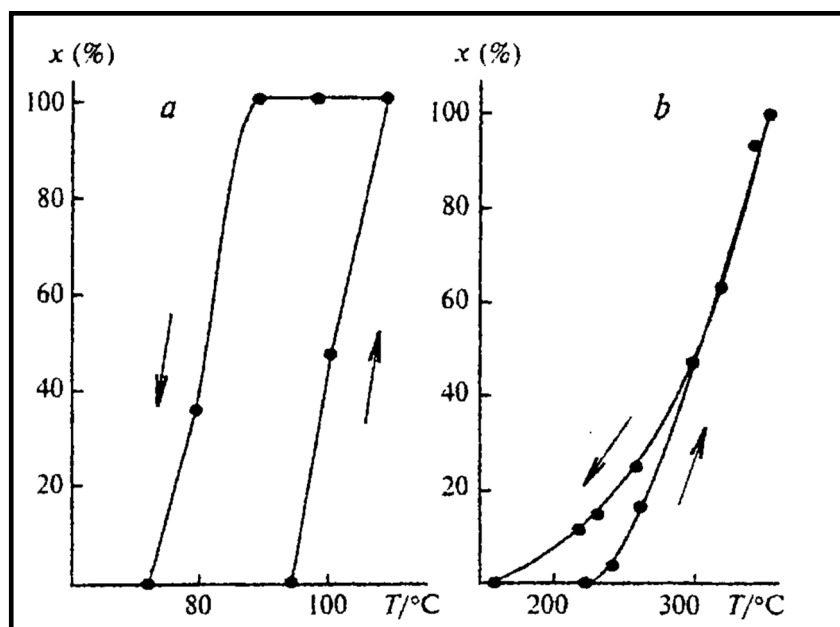


Figure 4. Hysteresis behavior during CO oxidation over unsupported copper oxide (CuO) (a) and over Pt foil (b) (the arrows mark the increase and the decrease in temperature) [63].

Carlsson et al. have studied oxidation of CO mixture in excess oxygen over Pt/Al₂O₃ and Pt/CeO₂ catalysts with the platinum phase distributed either homogeneously or heterogeneously in the support material using temperature-programmed experiments [5]. It has been found that the hysteresis width increases with decreasing CO concentrations, and at 0.1% CO, hysteresis is significantly broader for the heterogeneously distributed platinum catalysts compared to the homogeneously distributed Pt catalysts, as shown in Figure 5.

Furthermore, they studied the effect of the support in case of Pt/CeO₂ monolith catalysts. Results indicate that the width of the hysteresis does not change for CO concentrations, as shown in Figure 6 [5]. Lin et al. studied the hysteresis behavior of Pd/Al(OH)₃ and Pd/Mg(OH)₂ catalyst and found that Pd/Al(OH)₃ catalysts have smaller hysteresis compared to Pd/Mg(OH)₂ catalysts [135]. The porosity of catalyst support assumes a role in temperature hysteresis activity during CO oxidation reaction. For example, hysteresis was absent in Pt supported on non-porous titania catalyst (Pt/TiO₂), while Pt supported on porous silica (Pt/SiO₂) showed hysteresis [93,136,137].

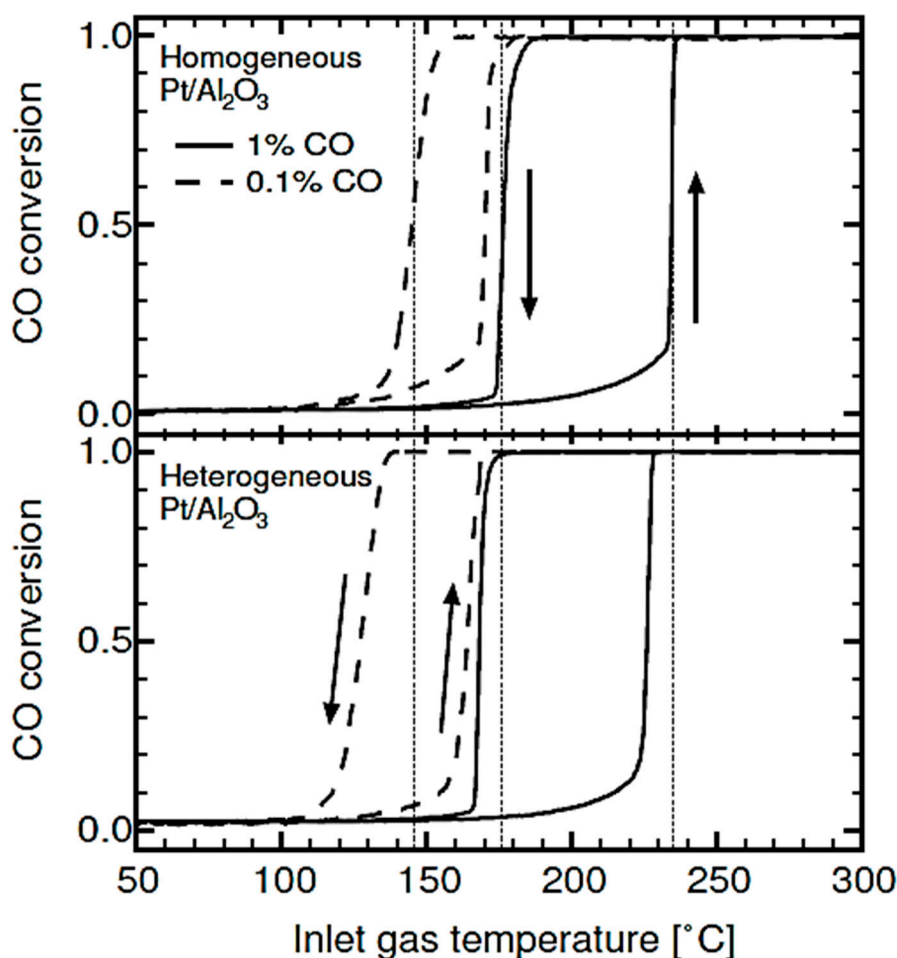


Figure 5. Temperature-programmed oxidation of 0.1 and 1% CO with 9% O₂ over homogeneous (top panel) and heterogeneous (bottom panel) Pt/Al₂O₃ monolith catalysts using heating/cooling rates of 5 °C/min [5].

Miller et al. reported hysteresis effect following pretreatment of Ru/RuO₂ catalyst that was attributed to arise from the changes in the catalyst structure [138]. Similar behavior was reported for CO oxidation on partially oxidized Pd nanoparticles, where slow hysteresis effects were found to depend on the pretreatment of catalyst samples [139]. Slavinskaya et al. [105] investigated the effect of structural and chemical states of palladium Pd/Al₂O₃ catalysts. They found that the destruction of large PdO particles and formation of smaller metallic palladium clusters resulted in the formation of core-shell structures, where the core was a PdO particle, and a shell formed by small PdO clusters, leading to self-sustained oscillations at different CO concentrations. The widening of hysteresis loop upon catalyst aging was attributed to morphological changes due to sintering of Pt particles, leading to different reduction and oxidation rates [55,94,140]. Casapu et al. investigated the effect of preparation method and the resulting morphological and structural properties of Pt nanoparticles, aging, temperature ramp rates, gas flows and CO concentrations on the hysteresis profile of CO oxidation for a Pt/Al₂O₃ catalyst (Figure 7) [94].

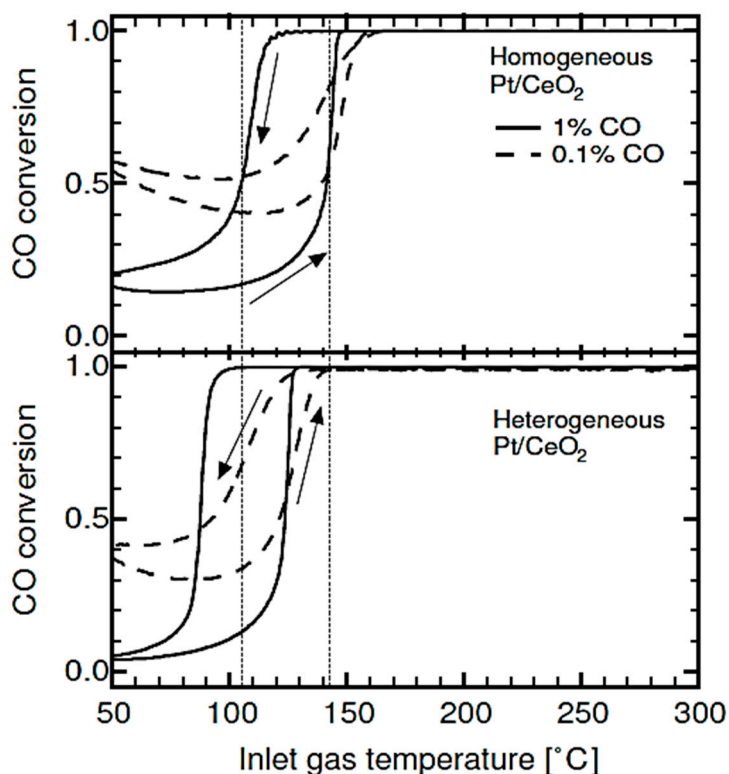


Figure 6. Temperature-programmed oxidation of 0.1 and 1% CO with 9% O₂ over homogeneous (top panel) and heterogeneous (bottom panel) Pt/CeO₂ monolith catalysts using heating/cooling rates of 5 °C/min [5].

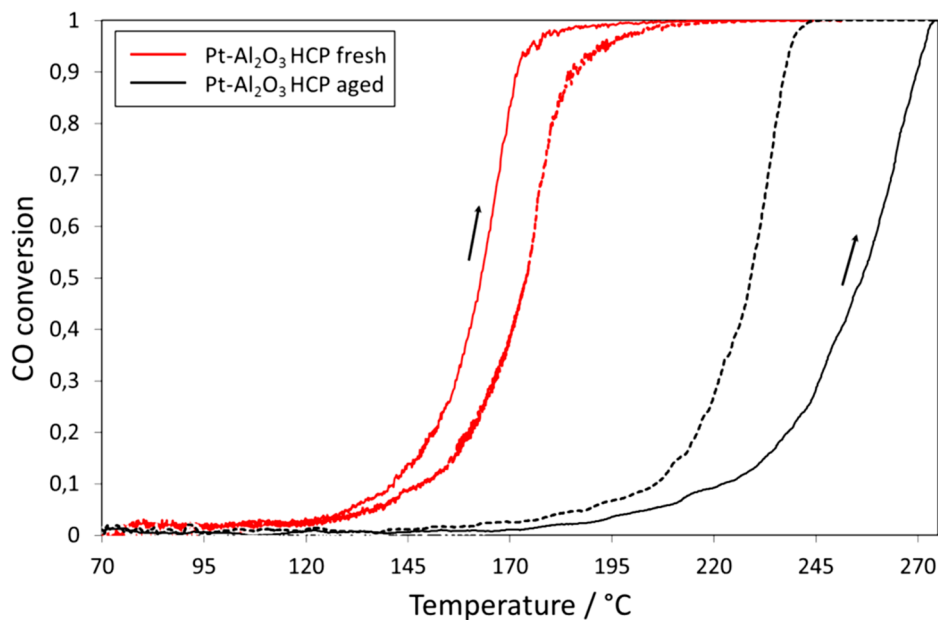


Figure 7. CO oxidation light-off (solid lines, indicated by the arrows) and light-out (dotted lines) over the Pt/Al₂O₃ catalyst before and after hydrothermal aging [94].

Heating and cooling rates and flow rates have been reported to affect hysteresis profiles [82]. Carlsson et al. reported that the hysteresis associated with the slow transition from an oxygen-enriched surface and platinum oxide formation during extinction, to a CO-covered surface including Pt reduction [55]. The different shape of hysteresis curves is attributed to inhibit accumulation of species on the surface during temperature ramp-up. Thermal inertia has been attributed to be responsible for

hysteresis effects in small-scale monolithic reactors [141]. Reduced activity during ignition process has been attributed to arise from CO poisoning and blocking of active sites at low temperatures. Hysteresis behavior is sensitive to local gas atmosphere, switching between normal and inverse hysteresis modes in complex gas mixtures. As a result, increased CO concentrations lead to a shift of the ignition toward higher temperatures due to the CO self-inhibition [5,54].

Differently-shaped hysteresis curves such as, normal, inverse or rectangular shape, occur due to inhibiting species accumulation on the surface during temperature ramp-up which was reported for nanocrystalline CuCr_2O_4 spinel catalysts in small-scale monolithic reactors, as shown in Figure 8. The small hysteresis is attributed to arise from high gas hourly space velocity (GHSV) of feed gas (60,000 mL/gh) which inhibits the formation of hot spots in the catalyst bed [142].

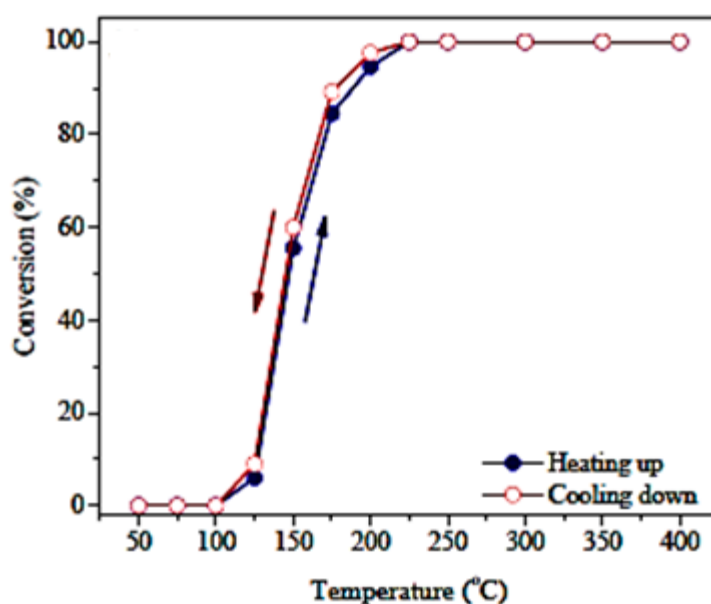


Figure 8. Hysteresis effect during CO oxidation on CuCr_2O_4 spinel catalyst. Very small hysteresis (almost none) observed [142].

Koutoufaris et al. used a model of the reactor behavior under transient conditions to investigate the effect of self-inhibition on the reaction propagation along the catalyst and its impact on hysteresis. Results revealed essential mechanisms related to the formation and role of surface intermediates or inhibitors on the hysteresis behavior during CO oxidation with an increase in the hysteresis width as a result of self-inhibition, as shown in Figure 9a [141].

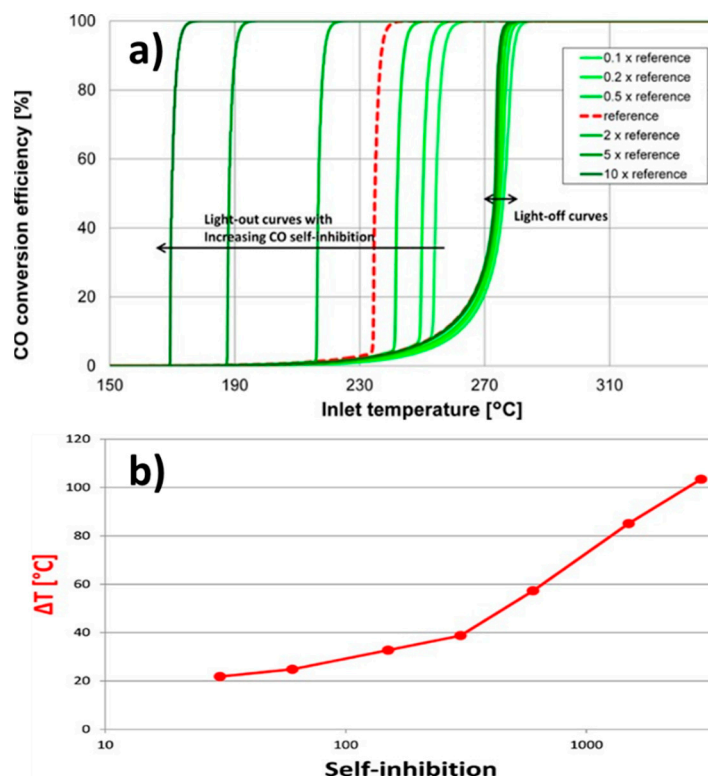


Figure 9. (a) Simulation results using different reaction and inhibition parameters. (b) Hysteresis magnitude as a function of self-inhibition parameter [141].

Mobini et al. reported inhibition effects on CuCr_2O_4 spinel catalyst [142]. It was reported that high feed gas concentration influenced increase or decrease in temperature for CO conversion, again arising due to inhibition of the formation of hot spots in the catalyst bed, as shown in Figure 9b, thus leading to a momentary transition from a high conversion to low conversion of CO oxidation reaction over this catalyst [142].

4. Analysis of Reviewed Literature

Hysteresis behavior is crucial for self-sustained low-temperature oxidation processes. Heterogeneous catalysts that exhibit hysteresis behavior over an extended temperature range are of primary importance. Several factors, such as particle size, gas pressure and the composition of gases, amongst others, decide the nature of catalyst suitable for use and the appropriate reaction conditions. Impurities on catalyst surfaces also affect the hysteresis behavior, as reported in the literature. Several studies report hysteresis for CO oxidation over a wide range of catalysts as summarized in Tables 1 and 2.

Table 1. Summary of the critical experiments which exhibited hysteresis.

Gas Used	Catalyst	Hysteresis Type	Reference
CO	Pt/Al ₂ O ₃	Normal	[5,30,85,94,114]
	Pt/TiO ₂ , Pt/SiO ₂	Normal	[93,136,137]
CO and CH ₄	Pt/Al ₂ O ₃ and Pt/CeO ₂	Inverse	[5,77,81]
CO	PdO/Al ₂ O ₃ , Pd/Al(OH) ₃ , Pd/Mg(OH) ₂	Normal	[105,135]
CO	Cu-Ce/ZSM-5 or CuCe _{1-x} Zr _x O _y /ZSM-5	Normal	[72,92]
CO	Unsupported Platinum wire, Platinum foil	Normal	[63,75]
CO, NO and C ₃ H ₆	Unsupported Platinum	Inverse	[5,49,54,67,91,111]
CO	Platinum and Palladium on alumina	Normal	[67,77,81–83]
CO	CuO	Normal	[63,117]
CO	Gold nanoparticles	Normal	[122–124]
CO	Ceria-supported catalyst with 0.28 wt% gold (Au), Germanium (Ge) and Gadolinium (Gd) dopants	Normal	[97,120,125]
CO	Pd/Ag, PdCu(110) alloys	Inverse	[95,96]
CO	Ru/RuO ₂	Normal	[138]

Table 2. Summary of the critical parameters and their effect on the exhibited hysteresis.

Parameter	Effect on Hysteresis Curve	Reference
Inlet CO concentration	Increasing CO concentration in inlet gas causes a higher light-off temperature or ignition point, the hysteresis loop increases upon increasing the CO concentrations	[52,56,74,77,87,126,142]
Inlet Temperature	Ignition and extinction shifted to higher temperatures with rapid increase in CO conversion	[77,128–134]
Surface Contamination and Aging	Increase in the hysteresis width due to the removal of contamination that blocks active sites	[75,94,141] [55,94,140]
Rate of temperature ramp-up	Increase in the temperature ramp-up result in shifting the ignition curve to higher temperatures	[72,92]
Inhibition parameters	Different inhibiting species accumulation on catalyst surface can change the shape of hysteresis curves and increase the width of the hysteresis.	[141,142].
Particle size	When the size decrease (less than 2 nm), the hysteresis changes from normal to inverse.	[68,94,124]

5. Conclusions

Hysteresis phenomena during CO oxidation has been studied intensively. However, explanations about its origin are conflicting as presented in the literature. Most of the experiments reported in the literature are scattered, and the range of catalysts and reactions used to study the hysteresis effect is minimal. Limited reports on hysteresis during CO oxidation relate this phenomenon to the structure and nature of the catalysts. Additionally, most of the data report the study of the CO conversion (%) as a function of the reactor inlet temperature instead of the reaction temperature, despite several studies discussing about creation of hotspots and the effect of reaction conditions and pretreatment conditions of catalysts. In order to improve the CO oxidation processes, a proper understanding of the conversion of CO is necessary.

The observed hysteresis phenomenon remains complex, and the reported literature is limited to specific catalysts or reaction parameters. New approaches are required to design and perform meaningful experiments. A systematic study of the hysteresis phenomenon on different catalysts should be conducted to answer many questions related to the effects of the wide range of reaction parameters, such as metal loading, pretreatment conditions, supports, aging, flow rate and heating rates. Based on the current trends surveyed in this review, the future probably has scope for further

progress and multidisciplinary efforts to come up with accurate explanations of this phenomenon that will certainly lead to other applications.

Author Contributions: R.M.A.S. wrote and edited the entire paper, K.M.S. oversaw the quality of the selected literature and the flow of the paper, and J.D. managed and participated in the quality of the manuscript. The authors worked together to prepare this manuscript. All authors read and approved this manuscript before submission.

Funding: This research received no external funding.

Conflicts of Interest: The authors declare no conflict of interest.

References

1. Heck, R.M.; Farrauto, R.J. Automobile exhaust catalysts. *Appl. Catal. A Gen.* **2001**, *221*, 443–457. [[CrossRef](#)]
2. Heck, R.M.; Farrauto, R.J.; Gulati, S.T. *Catalytic Air Pollution Control*; John Wiley & Sons, Inc.: Hoboken, NJ, USA, 2009. [[CrossRef](#)]
3. Kurz, H. Physiology of Angiogenesis. *J. Neurooncol.* **2000**, *50*, 17–35. [[CrossRef](#)]
4. Shelef, M.; McCabe, R.W. Twenty-five years after introduction of automotive catalysts: What next? *Catal. Today* **2000**, *62*, 35–50. [[CrossRef](#)]
5. Carlsson, P.-A.; Skoglundh, M. Low-temperature oxidation of carbon monoxide and methane over alumina and ceria supported platinum catalysts. *Appl. Catal. B Environ.* **2011**, *101*, 669–675. [[CrossRef](#)]
6. Prasad, R.; Singh, P. A Review on CO Oxidation Over Copper Chromite Catalyst. *Catal. Rev.* **2012**, *54*, 224–279. [[CrossRef](#)]
7. Manos, M.; James, A.D.; Amit, A.G.; Rahul, P.N.; Calvin, H.B.; Hu, Z.; Brian, C. *Atomic-Scale Design of iron Fisher-Tropsch Catalysts: A combined Computational Chemistry, Experimental, and Microkinetic Modeling Approach*; Office of Scientific and Technical Information (OSTI): Oak Ridge, TN, USA, 2005.
8. Wang, L.; Yang, L.; Zhang, Y.; Ding, W.; Chen, S.; Fang, W.; Yang, Y. Promoting effect of an aluminum emulsion on catalytic performance of Cu-based catalysts for methanol synthesis from syngas. *Fuel Process. Technol.* **2010**, *91*, 723–728. [[CrossRef](#)]
9. Grabow, L.C.; Gokhale, A.A.; Evans, S.T.; Dumesic, J.A.; Mavrikakis, M. Mechanism of the Water Gas Shift Reaction on Pt: First Principles, Experiments, and Microkinetic Modeling. *J. Phys. Chem. C* **2008**, *112*, 4608–4617. [[CrossRef](#)]
10. Armor, J.N. The multiple roles for catalysis in the production of H₂. *Appl. Catal. A Gen.* **1999**, *176*, 159–176. [[CrossRef](#)]
11. Kummer, J.T. Use of noble metals in automobile exhaust catalysts. *J. Phys. Chem.* **1986**, *90*, 4747–4752. [[CrossRef](#)]
12. Zhang, Y.; Wang, W. Recent advances in organocatalytic asymmetric Michael reactions. *Catal. Sci. Technol.* **2012**, *2*, 42–53. [[CrossRef](#)]
13. Yadav, R.; Saoud, k.; Rasouli, F.; Hajaligol, M. Formation and Deposition of Sputtered Nanoscale Particles in Cigarette Manufacture. U.S. Patent 8,051,859, 8 August 2005.
14. *Health Hazard Evaluation Determination Report: HHE-77-50-419, The Glass Detail, Cincinnati, Ohio, 45202*; U.S. Department of Health, Education, and Welfare, Public Health Service, Centers for Disease Control, National Institute for Occupational Safety and Health: Washington, DC, USA, 1977.
15. Henein, N.A.; Tagomori, M.K. Cold-start hydrocarbon emissions in port-injected gasoline engines. *Prog. Energy Combust. Sci.* **1999**, *25*, 563–593. [[CrossRef](#)]
16. Kašpar, J.; Fornasiero, P.; Hickey, N. Automotive catalytic converters: Current status and some perspectives. *Catal. Today* **2003**, *77*, 419–449. [[CrossRef](#)]
17. *Handbook of Heterogeneous Catalysis*; Wiley-VCH Verlag GmbH & Co. KGaA: Weinheim, Germany, 2008. [[CrossRef](#)]
18. Vannic, M.A. *Handbook of Heterogeneous Catalysis*. Herausgegeben von G. Ertl, H. Knözinger und]. Weitkamp, WILEY-VCH, Weinheim, 1997. 2500 S., geb., 24900.00 DM-ISBN 3-527-29212-8. *Angew. Chem.* **1997**, *109*, 2808–2810. [[CrossRef](#)]

19. Saoud, K.M. Supported gold nanocatalyst for low temperature CO oxidation and combustion of volatile organic compounds (VOC). In Proceedings of the Qatar Foundation Annual Research Forum Doha, Doha, Qatar, 13 December 2010.
20. Valange, S.; Védrine, J. General and Prospective Views on Oxidation Reactions in Heterogeneous Catalysis. *Catalysts* **2018**, *8*, 483. [[CrossRef](#)]
21. Comotti, M.; Weidenthaler, C.; Li, W.-C.; Schüth, F. Comparison of gold supported catalysts obtained by using different allotropic forms of titanium dioxide. *Top. Catal.* **2007**, *44*, 275–284. [[CrossRef](#)]
22. Beltramini, J.N.; Trimm, D.L. Role of germanium in bimetallic reforming catalysts. *React. Kinet. Catal. Lett.* **1988**, *37*, 293–299. [[CrossRef](#)]
23. Oh, S.; Hoflund, G. Low-temperature catalytic carbon monoxide oxidation over hydrous and anhydrous palladium oxide powders. *J. Catal.* **2007**, *245*, 35–44. [[CrossRef](#)]
24. Saoud, K.M. Carbon Monoxide Oxidation on Nanoparticle Catalysts and Gas Phase Reactions of Small Molecules and Volatile Organics with Metal Cations. Ph.D, Thesis, Virginia Commonwealth University, Richmond, VA, USA, 2005.
25. Boccuzzi, F.; Chiorino, A.; Tsubota, S.; Haruta, M. The oxidation and scrambling of CO with oxygen at room temperature on Au/ZnO. *Catal. Lett.* **1994**, *29*, 225–234. [[CrossRef](#)]
26. Escamilla-Perea, L.; Nava, R.; Pawelec, B.; Rosmaninho, M.G.; Peza-Ledesma, C.L.; Fierro, J.L.G. SBA-15-supported gold nanoparticles decorated by CeO₂: Structural characteristics and CO oxidation activity. *Appl. Catal. A Gen.* **2010**, *381*, 42–53. [[CrossRef](#)]
27. Keshipour, S.; Mirmasoudi, S.S. Cross-linked chitosan aerogel modified with Au: Synthesis, characterization and catalytic application. *Carbohydr. Polym.* **2018**, *196*, 494–500. [[CrossRef](#)]
28. Pan, F.; Zhang, W.; Ye, Y.; Huang, Y.; Xu, Y.; Yuan, Y.; Wu, F.; Li, J. Adsorption Synthesis of Iron Oxide-Supported Gold Catalyst under Self-Generated Alkaline Conditions for Efficient Elimination of Carbon Monoxide. *Catalysts* **2018**, *8*, 357. [[CrossRef](#)]
29. Reveles, J.U.; Saoud, K.M.; El-Shall, M.S. Water inhibits CO oxidation on gold cations in the gas phase. Structures and binding energies of the sequential addition of CO, H₂O, O₂, and N₂ onto Au⁺. *Phys. Chem. Chem. Phys.* **2016**, *18*, 28606–28616. [[CrossRef](#)] [[PubMed](#)]
30. Haaland, D. Simultaneous measurement of CO oxidation rate and surface coverage on Pt/Al₂O₃ using infrared spectroscopy: Rate hysteresis and CO island formation*1. *J. Catal.* **1982**, *76*, 450–465. [[CrossRef](#)]
31. Bond, G.C.; Thompson, D.T. Gold-catalysed oxidation of carbon monoxide. *Gold Bull.* **2000**, *33*, 41–50. [[CrossRef](#)]
32. Epling, W.S.; Hoflund, G.B.; Weaver, J.F.; Tsubota, S.; Haruta, M. Surface Characterization Study of Au/ α -Fe₂O₃ and Au/Co₃O₄ Low-Temperature CO Oxidation Catalysts. *J. Phys. Chem.* **1996**, *100*, 9929–9934. [[CrossRef](#)]
33. Haruta, M. Novel catalysis of gold deposited on metal oxides. *Catal. Surv. Jpn.* **1997**, *1*, 61–73. [[CrossRef](#)]
34. Haruta, M. Size- and support-dependency in the catalysis of gold. *Catal. Today* **1997**, *36*, 153–166. [[CrossRef](#)]
35. Montes, M.; Genet, M.; Hodnett, B.K.; Stone, W.E.; Delmon, B. X-Ray Photoelectron Spectroscopy of Sulfur Containing Ni/SiO₂ Catalysts. *Bull. Soc. Chim. Belg.* **2010**, *95*, 1–12. [[CrossRef](#)]
36. Yang, Y.; Saoud, K.M.; Abdelsayed, V.; Glaspell, G.; Deevi, S.; El-Shall, M.S. Vapor phase synthesis of supported Pd, Au, and unsupported bimetallic nanoparticle catalysts for CO oxidation. *Catal. Commun.* **2006**, *7*, 281–284. [[CrossRef](#)]
37. Abdelsayed, V.; Saoud, K.M.; El-Shall, M.S. Vapor phase synthesis and characterization of bimetallic alloy and supported nanoparticle catalysts. *J. Nanopart. Res.* **2006**, *8*, 519–531. [[CrossRef](#)]
38. El-Shall, M.S.; Saoud, K.M. Vapor Phase Synthesis of Gold Nanoparticle Catalysts for Low Temperature CO Oxidation. In Proceedings of the ACS 56th Southeast Regional Meeting, Research Triangle Park, NC, USA, 10–13 November 2004.
39. Glaspell, G.; Abdelsayed, V.; Saoud, K.M.; El-Shall, M.S. Vapor-phase synthesis of metallic and intermetallic nanoparticles and nanowires: Magnetic and catalytic properties. *Pure Appl. Chem.* **2006**, *78*, 1667–1689. [[CrossRef](#)]
40. Liu, W.; Flytzanistephanopoulos, M. Total Oxidation of Carbon Monoxide and Methane over Transition Metal Fluorite Oxide Composite Catalysts. *J. Catal.* **1995**, *153*, 304–316. [[CrossRef](#)]
41. Luo, M.-F.; Zhong, Y.-J.; Yuan, X.-X.; Zheng, X.-M. TPR and TPD studies of CuOCeO₂ catalysts for low temperature CO oxidation. *Appl. Catal. A Gen.* **1997**, *162*, 121–131. [[CrossRef](#)]

42. Martínez-Arias, A.; Soria, J.; Cataluña, R.; Conesa, J.C.; Corberán, V.C. Influence of Ceria Dispersion on the Catalytic Performance of Cu/(CeO₂)/Al₂O₃ Catalysts for the CO Oxidation Reaction. In *Catalysis and Automotive Pollution Control IV, Proceedings of the Fourth International Symposium (CAPoC4)*; Elsevier: Amsterdam, The Netherlands, 1998; pp. 591–600. [CrossRef]
43. Mergler, Y.J.; Hoebink, J.; Nieuwenhuys, B.E. CO Oxidation over a Pt/CoOx/SiO₂ Catalyst: A Study Using Temporal Analysis of Products. *J. Catal.* **1997**, *167*, 305–313. [CrossRef]
44. Biabani-Ravandi, A.; Rezaei, M.; Fattah, Z. Study of Fe-Co mixed metal oxide nanoparticles in the catalytic low-temperature CO oxidation. *Process Saf. Environ. Prot.* **2013**, *91*, 489–494. [CrossRef]
45. Yu, H.; Zhong, S.; Zhu, B.; Huang, W.; Zhang, S. Synthesis and CO Oxidation Activity of 1D Mixed Binary Oxide CeO₂-LaO (x) Supported Gold Catalysts. *Nanoscale Res. Lett.* **2017**, *12*, 579. [CrossRef]
46. Bonzel, H.P.; Ku, R. Carbon Monoxide Oxidation on a Pt(110) Single Crystal Surface. *J. Vac. Sci. Technol.* **1972**, *9*, 663–667. [CrossRef]
47. Cant, N. Steady-state oxidation of carbon monoxide over supported noble metals with particular reference to platinum. *J. Catal.* **1978**, *54*, 372–383. [CrossRef]
48. Dabill, D. The oxidation of hydrogen and carbon monoxide mixtures over platinum. *J. Catal.* **1978**, *53*, 164–167. [CrossRef]
49. Hegedus, L.L.; Oh, S.H.; Baron, K. Multiple steady states in an isothermal, integral reactor: The catalytic oxidation of carbon monoxide over platinum-alumina. *AIChE J.* **1977**, *23*, 632–642. [CrossRef]
50. Hoebink, J.H.B.J.; Nievergeld, A.J.L.; Marin, G.B. CO oxidation in a fixed bed reactor with high frequency cycling of the feed. *Chem. Eng. Sci.* **1999**, *54*, 4459–4468. [CrossRef]
51. Hori, G. Transient kinetics in CO oxidation on platinum. *J. Catal.* **1975**, *38*, 335–350. [CrossRef]
52. Salomons, S.; Hayes, R.E.; Votsmeier, M.; Drochner, A.; Vogel, H.; Malmberg, S.; Gieshoff, J. On the use of mechanistic CO oxidation models with a platinum monolith catalyst. *Appl. Catal. B Environ.* **2007**, *70*, 305–313. [CrossRef]
53. Voltz, S.E.; Morgan, C.R.; Liederman, D.; Jacob, S.M. Kinetic Study of Carbon Monoxide and Propylene Oxidation on Platinum Catalysts. *Ind. Eng. Chem. Prod. Res. Dev.* **1973**, *12*, 294–301. [CrossRef]
54. Salomons, S.; Votsmeier, M.; Hayes, R.E.; Drochner, A.; Vogel, H.; Gieshof, J. CO and H₂ oxidation on a platinum monolith diesel oxidation catalyst. *Catal. Today* **2006**, *117*, 491–497. [CrossRef]
55. Carlsson, P.; Osterlund, L.; Thormahlen, P.; Palmqvist, A.; Fridell, E.; Jansson, J.; Skoglundh, M. A transient in situ FTIR and XANES study of CO oxidation over Pt/AlO catalysts. *J. Catal.* **2004**, *226*, 422–434. [CrossRef]
56. Chakrabarty, T.; Silveston, P.L.; Hudgins, R.R. Hysteresis phenomena in co oxidation over platinum-alumina catalyst. *Can. J. Chem. Eng.* **1984**, *62*, 651–660. [CrossRef]
57. Imbihl, R.; Ertl, G. Oscillatory Kinetics in Heterogeneous Catalysis. *Chem. Rev.* **1995**, *95*, 697–733. [CrossRef]
58. Hysteresis. Available online: <https://en.wikipedia.org/wiki/Hysteresis> (accessed on 12 October 2018).
59. Noori, H.R. Examples of Hysteresis Phenomena in Biology. In *SpringerBriefs in Applied Sciences and Technology*; Springer: Berlin/Heidelberg, Germany, 2013; pp. 35–45. [CrossRef]
60. Visintin, A. Differential Models of Hysteresis. In *Applied Mathematical Sciences*; Springer: Berlin/Heidelberg, Germany, 1994. [CrossRef]
61. Haul, R.S.J.; Gregg, K.S.W. Sing: Adsorption, Surface Area and Porosity. 2. Auflage, Academic Press, London 1982. 303 Seiten, Preis: \$ 49.50. *Berichte Bunsengesellschaft Physikalische Chemie* **1982**, *86*, 957. [CrossRef]
62. Farrauto, R.J.; Lampert, J.K.; Hobson, M.C.; Waterman, E.M. Thermal decomposition and reformation of PdO catalysts; support effects. *Appl. Catal. B Environ.* **1995**, *6*, 263–270. [CrossRef]
63. Subbotin, A.N.; Gudkov, B.S.; Yakerson, V.I. Temperature hysteresis phenomena in heterogeneous catalysis. *Russ. Chem. Bull.* **2000**, *49*, 1373–1379. [CrossRef]
64. Kalinkin, A.V.; Boreskov, G.K.; Savchenko, V.I.; Dadayan, K.A. Study of CO oxidation on the (111) face of nickel during Ni-NiO phase transition. *React. Kinet. Catal. Lett.* **1980**, *13*, 111–114. [CrossRef]
65. Orlik, S.N.; Koval, G.L.; Fesenko, A.V.; Korneichuk, G.P.; Yablonskii, G.S. Kinetics of CO oxidation on a palladium-containing catalyst. *Theor. Exp. Chem.* **1979**, *15*, 59–61. [CrossRef]
66. Gudkov, B.S.; Subbotin, A.N.; Yakerson, V.I. On the phenomena of temperature hysteresis in hydrogenation reactions over heterogeneous catalysts. *React. Kinet. Catal. Lett.* **1999**, *68*, 125–132. [CrossRef]
67. Hauptmann, W.; Votsmeier, M.; Gieshoff, J.; Drochner, A.; Vogel, H. Inverse hysteresis during the NO oxidation on Pt under lean conditions. *Appl. Catal. B Environ.* **2009**, *93*, 22–29. [CrossRef]

68. Oh, S.; Baron, K.; Sloan, E.; Hegedus, L. Effects of catalyst particle size on multiple steady states. *J. Catal.* **1979**, *59*, 272–277. [[CrossRef](#)]
69. Schmitz, R.A. Multiplicity, Stability, and Sensitivity of States in Chemically Reacting Systems—A Review. In *Chemical Reaction Engineering Reviews*; American Chemical Society: Washington, DC, USA, 1975; pp. 156–211. [[CrossRef](#)]
70. Smith, T.G.; Zahradnik, J.; Carberry, J.J. Non-isothermal inter-intraphase effectiveness factors for negative order kinetics—CO oxidation over Pt. *Chem. Eng. Sci.* **1975**, *30*, 763–767. [[CrossRef](#)]
71. Subbotin, A.N.; Gudkov, B.S.; Dykh, Z.L.; Yakerson, V.I. Temperature hysteresis in CO oxidation on catalysts of various nature. *React. Kinet. Catal. Lett.* **1999**, *66*, 97–104. [[CrossRef](#)]
72. Usachev, N.Y.; Gorevaya, I.A.; Belanova, E.P.; Kazakov, A.V.; Kharlamov, V.V. Hysteresis phenomenon in CO and hydrogen oxidation on Cu-Ce-Zr-O systems. *Mendeleev Commun.* **2004**, *14*, 79–80. [[CrossRef](#)]
73. Wei, J.; Becker, E.R. The Optimum Distribution of Catalytic Material on Support Layers in Automotive Catalysis. In *Advances in Chemistry*; American Chemical Society: Washington, DC, USA, 1975; pp. 116–132. [[CrossRef](#)]
74. Ye, S.; Yap, Y.H.; Kolaczowski, S.T.; Robinson, K.; Lukyanov, D. Catalyst ‘light-off’ experiments on a diesel oxidation catalyst connected to a diesel engine—Methodology and techniques. *Chem. Eng. Res. Des.* **2012**, *90*, 834–845. [[CrossRef](#)]
75. Engel, T.; Ertl, G. Elementary Steps in the Catalytic Oxidation of Carbon Monoxide on Platinum Metals. In *Advance Catalysis*; Academic Press: Cambridge, MA, USA, 1979; Volume 28, pp. 1–78. [[CrossRef](#)]
76. Salanov, A.N.; Savchenko, V.I. TD and AES studies of the interaction of oxygen with Rh(100). *React. Kinet. Catal. Lett.* **1985**, *29*, 101–109. [[CrossRef](#)]
77. Abedi, A.; Hayes, R.; Votsmeier, M.; Epling, W.S. Inverse Hysteresis Phenomena During CO and C₃H₆ Oxidation over a Pt/Al₂O₃ Catalyst. *Catal. Lett.* **2012**, *142*, 930–935. [[CrossRef](#)]
78. Busca, G.; Cristiani, C.; Forzatti, P.; Groppi, G. Surface characterization of Ba- γ -alumina. *Catal. Lett.* **1995**, *31*, 65–74. [[CrossRef](#)]
79. Dalle Nogare, D.; Salemi, S.; Biasi, P.; Canu, P. Taking advantage of hysteresis in methane partial oxidation over Pt on honeycomb monolith. *Chem. Eng. Sci.* **2011**, *66*, 6341–6349. [[CrossRef](#)]
80. McCarty, J.G. Kinetics of PdO combustion catalysis. *Catal. Today* **1995**, *26*, 283–293. [[CrossRef](#)]
81. Amin, A.; Abedi, A.; Hayes, R.; Votsmeier, M.; Epling, W. Methane oxidation hysteresis over Pt/Al₂O₃. *Appl. Catal. A Gen.* **2014**, *478*, 91–97. [[CrossRef](#)]
82. Dadi, R.K.; Luss, D.; Balakotiah, V. Dynamic hysteresis in monolith reactors and hysteresis effects during co-oxidation of CO and C₂H₆. *Chem. Eng. J.* **2016**, *297*, 325–340. [[CrossRef](#)]
83. Etheridge, J.E.; Watling, T.C. Is reactor light-off data sufficiently discriminating between kinetic parameters to be used for developing kinetic models of automotive exhaust aftertreatment catalysts? The effect of hysteresis induced by strong self inhibition. *Chem. Eng. J.* **2015**, *264*, 376–388. [[CrossRef](#)]
84. Sun, M.; Croiset, E.B.; Hudgins, R.R.; Silveston, P.L.; Menzinger, M. Steady-State Multiplicity and Superadiabatic Extinction Waves in the Oxidation of CO/H₂Mixtures over a Pt/Al₂O₃-Coated Monolith. *Ind. Eng. Chem. Res.* **2003**, *42*, 37–45. [[CrossRef](#)]
85. Bourane, A.; Bianchi, D. Oxidation of CO on a Pt/Al₂O₃ Catalyst: From the Surface Elementary Steps to Lighting-Off Tests. *J. Catal.* **2002**, *209*, 126–134. [[CrossRef](#)]
86. Russell, A.; Epling, W.S.; Hess, H.; Chen, H.-Y.; Henry, C.; Currier, N.; Yezerets, A. Spatially-Resolved Temperature and Gas Species Changes in a Lean-Burn Engine Emissions Control Catalyst. *Ind. Eng. Chem. Res.* **2010**, *49*, 10311–10322. [[CrossRef](#)]
87. Chakrabarty, T.; Hudgins, R.R.; Silveston, P.L. Criterion for simultaneous interphase temperature and concentration gradients. *J. Chem. Eng. Jpn.* **1982**, *15*, 237–239. [[CrossRef](#)]
88. Depcik, C.; Loya, S.; Srinivasan, A.; Wentworth, T.; Stagg-Williams, S. Adaptive Global Carbon Monoxide Kinetic Mechanism over Platinum/Alumina Catalysts. *Catalysts* **2013**, *3*, 517–542. [[CrossRef](#)]
89. Poenitzsch, L.; Wilde, M.; Tetenyi, P.; Dobrovolszky, M.; Paal, Z. ChemInform Abstract: Sulfur Adsorption, Desorption, and Exchange on Platinum/Alumina, Rhenium/Alumina, and Platinum-Rhenium/Alumina Catalysts. *ChemInform* **2010**, *23*. [[CrossRef](#)]
90. Pakharukov, I.Y.; Stakheev, A.Y.; Beck, I.E.; Zubavichus, Y.V.; Murzin, V.Y.; Parmon, V.N.; Bukhtiyarov, V.I. Concentration Hysteresis in the Oxidation of Methane over Pt/ γ -Al₂O₃: X-ray Absorption Spectroscopy and Kinetic Study. *ACS Catal.* **2015**, *5*, 2795–2804. [[CrossRef](#)]

91. Dubbe, H.; Eigenberger, G.; Nieken, U. Hysteresis Phenomena on Pt- and Pd-Diesel Oxidation Catalysts: Experimental Observations. *Top. Catal.* **2016**, *59*, 1054–1058. [[CrossRef](#)]
92. Zhao, R.; Hao, Q.; Bin, F.; Kang, R.; Dou, B. Influence of Ce/Zr Ratio on the Synergistic Effect over CuCe_{1-x}Zr_xO_y/ZSM-5 Catalysts for the Self-Sustained Combustion of Carbon Monoxide. *Combust. Sci. Technol.* **2017**, *189*, 1394–1415. [[CrossRef](#)]
93. Hlaváček, V.; Votruba, J. Hysteresis and Periodic Activity Behavior in Catalytic Chemical Reaction Systems. In *Advances in Catalysis*; Academic Press: Cambridge, MA, USA, 1979; Volume 27, pp. 59–96. [[CrossRef](#)]
94. Casapu, M.; Fischer, A.; Gänzler, A.M.; Popescu, R.; Crone, M.; Gerthsen, D.; Türk, M.; Grunwaldt, J.-D. Origin of the Normal and Inverse Hysteresis Behavior during CO Oxidation over Pt/Al₂O₃. *ACS Catal.* **2016**, *7*, 343–355. [[CrossRef](#)]
95. Mousa, M.S.; Hammoudeh, A.; Loboda-Cackovic, J.; Block, J.H. The CO-oxidation on Pd-rich surfaces of PdCu(110): Hysteresis in reaction rates. *J. Mol. Catal. A Chem.* **1995**, *96*, 271–276. [[CrossRef](#)]
96. Fernandes, V.R.; Bossche, M.V.d.; Knudsen, J.; Farstad, M.H.; Gustafson, J.; Venvik, H.J.; Grönbeck, H.; Borg, A. Reversed Hysteresis during CO Oxidation over Pd₇₅Ag₂₅(100). *ACS Catal.* **2016**, *6*, 4154–4161. [[CrossRef](#)]
97. Deng, W.; Jesus, J.D.; Saltsburg, H.; Flytzani-Stephanopoulos, M. Low-content gold-ceria catalysts for the water-gas shift and preferential CO oxidation reactions. *Appl. Catal. A Gen.* **2005**, *291*, 126–135. [[CrossRef](#)]
98. Beusch, H.; Fieguth, P.; Wicke, E. Thermisch und kinetisch verursachte Instabilitäten im Reaktionsverhalten einzelner Katalysatorkörner. *Chem. Ing. Tech.* **1972**, *44*, 445–451. [[CrossRef](#)]
99. Roberts, G.W.; Satterfield, C.N. Effectiveness Factor for Porous Catalysts. Langmuir-Hinshelwood Kinetic Expressions for Bimolecular Surface Reactions. *Ind. Eng. Chem. Fundam.* **1966**, *5*, 317–325. [[CrossRef](#)]
100. Schneider, P.; Mitschka, P. Effect of internal diffusion on catalytic reactions. IV. Reversible second-order reaction with Langmuir-Hinshelwood type of rate equation. *Collect. Czechoslov. Chem. Commun.* **1966**, *31*, 3677–3701. [[CrossRef](#)]
101. Luss, D.; Lee, J.C.M. Stability of an isothermal catalytic reaction with complex rate expression. *Chem. Eng. Sci.* **1971**, *26*, 1433–1443. [[CrossRef](#)]
102. Padberg, G.; Wicke, E. Stabiles und instabiles Verhalten eines adiabatischen Rohrreaktors am Beispiel der katalytischen CO-Oxydation. *Chem. Eng. Sci.* **1967**, *22*, 1035–1051. [[CrossRef](#)]
103. Cutlip, M.B.; Kenney, C.N. Limit Cycle Phenomena during Catalytic Oxidation Reactions over a Supported Platinum Catalyst. In *ACS Symposium Series*; American Chemical Society: Washington, DC, USA, 1978; pp. 475–486. [[CrossRef](#)]
104. Ekerdt, J.G. *Catalytic Hydrocarbon Reactions over Supported Metals. Progress Report, February 1, 1992–March 31, 1993*; No. DOE/ER/13604-22; Office of Scientific and Technical Information (OSTI): Oak Ridge, TN, USA, 1993. [[CrossRef](#)]
105. Lashina, E.A.; Slavinskaya, E.M.; Chumakova, N.A.; Stonkus, O.A.; Gulyaev, R.V.; Stadnichenko, A.I.; Chumakov, G.A.; Boronin, A.I.; Demidenko, G.V. Self-sustained oscillations in CO oxidation reaction on PdO/Al₂O₃ catalyst. *Chem. Eng. Sci.* **2012**, *83*, 149–158. [[CrossRef](#)]
106. Hlaváček, V.; Votruba, J. Experimental Study of Multiple Steady States in Adiabatic Catalytic Systems. In *Chemical Reaction Engineering—II*; American Chemical Society: Washington, DC, USA, 1975; Volume 133, pp. 545–558.
107. Saoud, K.; Al Soubaihi, R.; Dutta, J. Self-sustaining and hysteresis behavior of low-temperature CO oxidation on mesoporous Pd/SiO₂ aerogel s catalyst under dynamics conditions. In Proceedings of the 256th National Meeting and Exposition of the American-Chemical-Society (ACS)—Nanoscience, Nanotechnology and Beyond, Boston, MA, USA, 19–23 August 2018.
108. Al Soubaihi, R.M. Thermal Hysteresis of Palladium encaged inside Mesoporous Silica catalyst for Low Temperature CO oxidation. *Qatar Found. Annu Res. Conf. Proc.* **2018**, *2018*, EEPD363. [[CrossRef](#)]
109. Eigenberger, G. Kinetic instabilities in heterogeneously catalyzed reactions—I. *Chem. Eng. Sci.* **1978**, *33*, 1255–1261. [[CrossRef](#)]
110. Rathouský, J.; Kíra, E.; Hlaváček, V. Experimental observations of complex dynamic behavior in the catalytic oxidation of CO on Pt/alumina catalyst. *Chem. Eng. Sci.* **1981**, *36*, 781–782. [[CrossRef](#)]
111. Dauchot, J.P.; Cakenberghe, J.V. Oscillations during Catalytic Oxidation of Carbon Monoxide on Platinum. *Nat. Phys. Sci.* **1973**, *246*, 61–63. [[CrossRef](#)]

112. Hugo, P.; Jakubith, M. Dynamisches Verhalten und Kinetik der Kohlenmonoxid-Oxidation am Platin-Katalysator. *Chem. Ing. Tech.* **1972**, *44*, 383–387. [[CrossRef](#)]
113. Zahradnik, J.; McCarthy, E.F.; Kuczynski, G.C.; Carberry, J.J. Effect of Ambient Atmosphere on Sintering of $\alpha\text{Al}_2\text{O}_3$ Supported Pt Catalysts. In *Sintering and Catalysis*; Springer: Berlin, Germany, 1975; pp. 199–209. [[CrossRef](#)]
114. Boubnov, A.; Gänzler, A.; Conrad, S.; Casapu, M.; Grunwaldt, J.-D. Oscillatory CO Oxidation Over Pt/ Al_2O_3 Catalysts Studied by In situ XAS and DRIFTS. *Top. Catal.* **2013**, *56*, 333–338. [[CrossRef](#)]
115. Gänzler, A.M.; Casapu, M.; Boubnov, A.; Müller, O.; Conrad, S.; Lichtenberg, H.; Frahm, R.; Grunwaldt, J.-D. Operando spatially and time-resolved X-ray absorption spectroscopy and infrared thermography during oscillatory CO oxidation. *J. Catal.* **2015**, *328*, 216–224. [[CrossRef](#)]
116. Barth, J. Transport of adsorbates at metal surfaces: From thermal migration to hot precursors. *Surf. Sci. Rep.* **2000**, *40*, 75–149. [[CrossRef](#)]
117. Subbotin, A.N.; Gudkov, B.S.; Yakerson, V.I.; Chertkova, S.V.; Golosman, E.Z.; Kozyreva, G.V. Temperature-Hysteresis Effects in CO Oxidation on Cement Catalysts with Various CuO Content. *Russ. J. Appl. Chem.* **2001**, *74*, 1506–1508. [[CrossRef](#)]
118. Frank-Kamenetskii, D.A. *Diffusion and Heat Exchange in Chemical Kinetics*; Princeton University Press: Princeton, NJ, USA, 1955. [[CrossRef](#)]
119. Subbotin, A.N.; Subbotina, I.R.; Golosman, E.Z. Hysteresis phenomena in heterogeneous exothermal catalytic reactions and methods for decreasing the overheating of catalyst nanoclusters. *Mendeleev Commun.* **2015**, *25*, 216–218. [[CrossRef](#)]
120. Yuranov, I.; Kiwi-Minsker, L.; Slin'ko, M.; Kurkina, E.; Tolstunova, E.D.; Renken, A. Oscillatory behavior during CO oxidation over Pd supported on glass fibers: Experimental study and mathematical modeling. *Chem. Eng. Sci.* **2000**, *55*, 2827–2833. [[CrossRef](#)]
121. Ishchenko, E.V.; Yatsimirskii, V.K.; Gaidai, S.V. Temperature Hysteresis in Oxidation of CO on Complex Oxide Catalysts. *Theor. Exp. Chem.* **2005**, *41*, 340–345. [[CrossRef](#)]
122. Kipnis, M. Gold in CO oxidation and PROX: The role of reaction exothermicity and nanometer-scale particle size. *Appl. Catal. B Environ.* **2014**, *152–153*, 38–45. [[CrossRef](#)]
123. Kipnis, M.; Volnina, E. New approaches to preferential CO oxidation over noble metals. *Appl. Catal. B Environ.* **2010**, *98*, 193–203. [[CrossRef](#)]
124. Rozovskii, A.Y.; Kipnis, M.A.; Volnina, E.A.; Lin, G.I.; Samokhin, P.V. Selective oxidation of CO under conditions of catalyst surface ignition. *Kinet. Catal.* **2007**, *48*, 701–710. [[CrossRef](#)]
125. Lindstrom, T.H.; Tsotsis, T.T. Reaction rate oscillations during CO oxidation over Pt/ $\gamma\text{-Al}_2\text{O}_3$; experimental observations and mechanistic causes. *Surf. Sci.* **1985**, *150*, 487–502. [[CrossRef](#)]
126. Yablonskii, G.S.; Lazman, M.Z. New correlations to analyze isothermal critical phenomena in heterogeneous catalysis reactions (“Critical simplification”, “hysteresis thermodynamics”). *React. Kinet. Catal. Lett.* **1996**, *59*, 145–150. [[CrossRef](#)]
127. Newton, M. Time Resolved Operando X-ray Techniques in Catalysis, a Case Study: CO Oxidation by O₂ over Pt Surfaces and Alumina Supported Pt Catalysts. *Catalysts* **2017**, *7*, 58. [[CrossRef](#)]
128. Epling, W.S.; Campbell, L.E.; Yezerets, A.; Currier, N.W.; Parks, J.E. Overview of the Fundamental Reactions and Degradation Mechanisms of NO_x Storage/Reduction Catalysts. *Catal. Rev.* **2004**, *46*, 163–245. [[CrossRef](#)]
129. Farrauto, R.J.; Heck, R.M. Catalytic converters: State of the art and perspectives. *Catal. Today* **1999**, *51*, 351–360. [[CrossRef](#)]
130. Havenith, C.; Verbeek, R.P. Transient Performance of a Urea deNO_x Catalyst for Low Emissions Heavy-Duty Diesel Engines. In *Proceedings of the SAE Technical Paper Series*; SAE: Warrendale, PA, USA, 1997. [[CrossRef](#)]
131. Held, W.; König, A.; Richter, T.; Puppe, L. Catalytic NO_x Reduction in Net Oxidizing Exhaust Gas. I. *SAE Trans.* **1990**, *99*, 209–216.
132. Jung, J.; Song, S.; Chun, K.M. Characterization of Catalyzed Soot Oxidation with NO₂, NO and O₂ using a Lab-Scale Flow Reactor System. In *Proceedings of the SAE Technical Paper Series*; SAE: Warrendale, PA, USA, 2008. [[CrossRef](#)]
133. Salasc, S.; Skoglundh, M.; Fridell, E. A comparison between Pt and Pd in NO_x storage catalysts. *Appl. Catal. B Environ.* **2002**, *36*, 145–160. [[CrossRef](#)]

134. Tronci, S.; Baratti, R.; Gavriilidis, A. Catalytic converter design for minimisation of cold-start emissions. *Chem. Eng. Commun.* **1999**, *173*, 53–77. [[CrossRef](#)]
135. Lin, X.; Zhou, J.; Fan, Y.; Zhan, Y.; Chen, C.; Li, D.; Jiang, L. Mg-Al hydrotalcite-supported Pd catalyst for low-temperature CO oxidation: Effect of Pdⁿ⁺ species and surface hydroxyl groups. *Dalton Trans.* **2018**. [[CrossRef](#)] [[PubMed](#)]
136. Berzins, A.R.; Vong, M.S.W.L.; Sermon, P.A.; Wurie, A.T. Isothermal Chemisorption upon Oxide-Supported Platinum. *Adsorpt. Sci. Technol.* **1984**, *1*, 51–76. [[CrossRef](#)]
137. Kiwi-Minsker, L.; Yuranov, I.; Siebenhaar, B.; Renken, A. Glass fiber catalysts for total oxidation of CO and hydrocarbons in waste gases. *Catal. Today* **1999**, *54*, 39–46. [[CrossRef](#)]
138. Miller, B.K.; Crozier, P.A. Operando TEM of Ru/RuO₂ Catalyst Performing CO Oxidation. *Microsc. Microanal.* **2014**, *20*, 1564–1565. [[CrossRef](#)]
139. Schalow, T.; Brandt, B.; Laurin, M.; Schauermaun, S.; Libuda, J.; Freund, H. CO oxidation on partially oxidized Pd nanoparticles. *J. Catal.* **2006**, *242*, 58–70. [[CrossRef](#)]
140. Hauptmann, W.; Votsmeier, M.; Vogel, H.; Vlachos, D.G. Modeling the simultaneous oxidation of CO and H₂ on Pt—Promoting effect of H₂ on the CO-light-off. *Appl. Catal. A Gen.* **2011**, *397*, 174–182. [[CrossRef](#)]
141. Koutoufaris, I.; Koltsakis, G. Heat- and mass-transfer induced hysteresis effects during catalyst light-off testing. *Can. J. Chem. Eng.* **2014**, *92*, 1561–1569. [[CrossRef](#)]
142. Mobini, S.; Meshkani, F.; Rezaei, M. Surfactant-assisted hydrothermal synthesis of CuCr₂O₄ spinel catalyst and its application in CO oxidation process. *J. Environ. Chem. Eng.* **2017**, *5*, 4906–4916. [[CrossRef](#)]



© 2018 by the authors. Licensee MDPI, Basel, Switzerland. This article is an open access article distributed under the terms and conditions of the Creative Commons Attribution (CC BY) license (<http://creativecommons.org/licenses/by/4.0/>).